HOKKAIDO UNIVERSITY

| | |
|---|---|
| Title | Float zone growth and spectral properties of Cr,Nd:CaYAlO4 single crystals |
| Author(s) | Ueda, Aki; Higuchi, Mikio; Yamada, Daiki et al. |
| Citation | Journal of Crystal Growth, 404, 152-156<br>https://doi.org/10.1016/j.jcrysgro.2014.07.027 |
| Issue Date | 2014-10-15 |
| Doc URL | https://hdl.handle.net/2115/57424 |
| Type | journal article |
| File Information | aper_revise.pdf |

Hokkaido University Collection of Scholarly and Academic Papers : HUSCAP

# Float zone growth and spectral properties of Cr,Nd:$CaYAlO_4$ single crystals

Aki Ueda[a], Mikio Higuchi[a,b,*], Daiki Yamada[a], Sho Namiki[b], Takayo Ogawa[b], Satoshi Wada[b], Kiyoharu Tadanaga[a]

[a]Faculty of Engineering, Hokkaido University, Sapporo 060-8628, Japan

[b]RIKEN, Wako 351-0198, Japan

*Corresponding author

Phone: +81-11-706-6573

E-mail: hig@eng.hokudai.ac.jp

Abstract

Cr,Nd:$CaYAlO_4$ single crystals were grown by the floating zone method and their spectroscopic properties were investigated. Many voids were observed in the crystals grown with a stoichiometric feed rod even at a relatively low growth rate of 2.5 mm/h, while a void-free crystal was grown at the same growth rate using a feed rod the composition of which was Y-rich to Ca. These results indicate that voids were

attributable to constitutional supercooling due to the segregation of main constituents caused by the difference in congruent and stoichiometric compositions. The as-grown crystals were deep red and showed strong absorption in the wavelength region of 320-600 nm. The absorption cross section for σ-polarization at 430 nm, where Cr,Nd:YAG has the maximum absorption, is about 1160 $\times 10^{-20}$ $cm^2$, which is 165 times as large as that of Cr,Nd:YAG. By pumping at 400 nm, which is a part of the absorption band of $Cr^{3+}$, Cr,Nd:$CaYAlO_4$ showed fluorescence bands around 900 nm and 1080 nm by $Nd^{3+}$ indicating energy transfer from $Cr^{3+}$ to $Nd^{3+}$ in the crystal. Cr,Nd:$CaYAlO_4$ single crystals are therefore one of the promising gain media for solar-pumped solid state laser systems.

## Highlights

- $Cr,Nd:CaYAlO_4$ single crystals were grown by the floating zone method.
- Void formation is attributable to the segregation between Ca and Y species.
- Absorption cross-section of $Cr,Nd:CaYAlO_4$ for σ-polarizaionwas about $1160 \times 10^{-20}$ $cm^2$.
- Emission bands of $Nd^{3+}$ were observed with the excitation at 400 nm.


## Keywords

A1 Defects

A2 Floating zone technique

B1 Aluminates

B3 Solid state lasers

## 1. Introduction

Depletion of fossil fuels will be one of the most serious problems in the future even though mining technologies are progressing, and efficient utilization of solar energy is therefore strongly required from the viewpoint of development of sustainable energy sources. Solar-pumped laser is one of the effective systems to utilize solar energy. Yabe et al. suggested a magnesium refining system using solar-pumped laser system [1] and succeeded to obtain an output of 80 W with YAG ceramic as a gain medium by pumping with converged solar radiation [2]. Hydrogen production using metal nanoparticles [3] or photocatalysts [4], and transmission of solar energy to the ground from space [5] are also possible applications of the solar-pumped lasers.

A number of candidate materials such as Nd-doped glass [6, 7] and oxide single crystals [8-10] have so far been developed as the gain media for solar- pumped lasers. Cr,Nd:YAG is one of the most investigated media [11], and the transparent YAG ceramic is mainly used in recent studies [12]. However, absorption of Cr,Nd:YAG around 500 nm which corresponds to the wavelength of solar radiation peak and the absorption cross section are relatively small even at the absorption peak wavelength. In addition, the garnet structure has four-fold coordination site and chromium can occupy the site as a tetravalent ion, $Cr^{4+}$, which shows a broad absorption band in the

near-infrared region where $Nd^{3+}$ emission bands are present resulting in reduced lasing performance [13].

In order to overcome these problems, we focused on $CaYAlO_4$ as a host crystal for $Cr^{3+}$ and $Nd^{3+}$. The structure of $CaYAlO_4$ is illustrated in Fig. 1. $CaYAlO_4$ adopts the $K_2NiF_4$ type structure, in which no tetrahedral site exists, and nine-fold coordinated Y site and six-fold coordinated Al site can be substituted by $Nd^{3+}$ ion and $Cr^{3+}$ ion, respectively. Due to the random distribution of $Ca^{2+}$ and $Y^{3+}$ in the structure [14], coordination environment of $Cr^{3+}$ is diversified, and broadening of the absorption band of $Cr^{3+}$ is consequently expected. In previous studies, laser oscillation was reported using a Nd:CaYAlO single crystal [15-17] and growth of $CaYAlO_4$ single crystals doped with other rare earth ions were investigated [18-22]. Cr:$CaYAlO_4$ was also synthesized and broad absorption bands in the visible region were observed [22, 23]. However, there has been no report on the growth and spectroscopic properties of Cr,Nd:$CaYAlO_4$ single crystals.

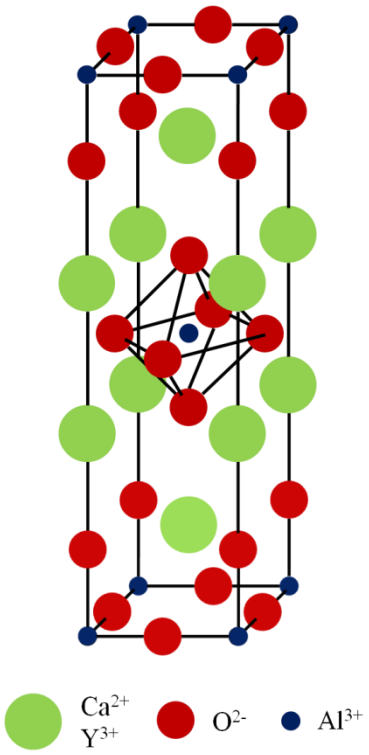


In this study, we tried float zone growth of Cr,Nd:$CaYAlO_4$ single crystal to

establish adequate growth conditions to obtain high quality single crystals which can be used as a laser medium and revealed spectroscopic properties of Cr,Nd:$CaYAlO_4$. On the basis of the obtained results, the potentiality of Cr,Nd:$CaYAlO_4$ single crystals as a solar pumped laser medium is discussed.

## 2. Experimental procedure

$CaCO_3$ (99.99%), $Y_2O_3$ (99.99%), $Nd_2O_3$ (99.9%), $Al_2O_3$ (99.99%) and $Cr_2O_3$ (99.98%) were used as starting materials. They were weighed according to the compositions shown in Table 1 and mixed in an alumina mortar with ethanol, followed by calcination in air at 1000 °C for 10 h. The calcined powder was ground and pressed into a rod under a hydrostatic pressure of 100 MPa. The rod was sintered in air at 1400 °C for 10 h and a feed rod was thus obtained. Cr,Nd:$CaYAlO_4$ single crystals were grown using an image furnace with

| Sample | Composition |
|---|---|
| Stoichiometry | $Ca(Y_{0.99}Nd_{0.01})(Al_{0.999}Cr_{0.001})O_4$ |
| Y-rich 0.5 mol% vs. Ca | $Ca_{0.9925}(Y_{0.99}Nd_{0.01})_{1.005}(Al_{0.999}Cr_{0.001})O_4$ |
| Al-rich 0.5 mol% vs. Y | $Ca(Y_{0.99}Nd_{0.01})_{0.995}(Al_{0.999}Cr_{0.001})_{1.005}O_4$ |

double ellipsoidal mirrors (SC-N35HD-L, NEC, infrared source: halogen lamp of 1.5 kW). The growth atmosphere was $O_2$, air, air / $N_2$ mixed gas, $CO_2$, or $N_2$ stream (2 L/h). The growth rate was 2.5-5 mm/h, and the rotation rate was 30-60 rpm for the seed crystal and 5 rpm for the feed.

A polarizing microscope (BX51, OLYMPUS and SZH-ILLB, OLYMPUS) was used to evaluate the quality of the grown crystals. Initial and end portions of the grown crystals were cut into discs and both sides of the discs were polished to be mirror finish. An X-ray diffractometer (RINT-2000 Ultima, Rigaku) was used to determine the lattice parameters of the grown crystals.

Polarized absorption spectra of the Cr,Nd:$CaYAlO_4$ were measured using a sample in which the c-axis was parallel to the surface with a spectrophotometer (UV-VIS-NIR scanning spectrophotometer, Shimadzu). Emission spectra were also measured with a fluorescence spectrophotometer (Fluolog®-3, HORIBA).

## 3. Results and discussion

### *3.1. Crystal growth*

Cr,Nd:$CaYAlO_4$ single crystals grown in various atmospheres are

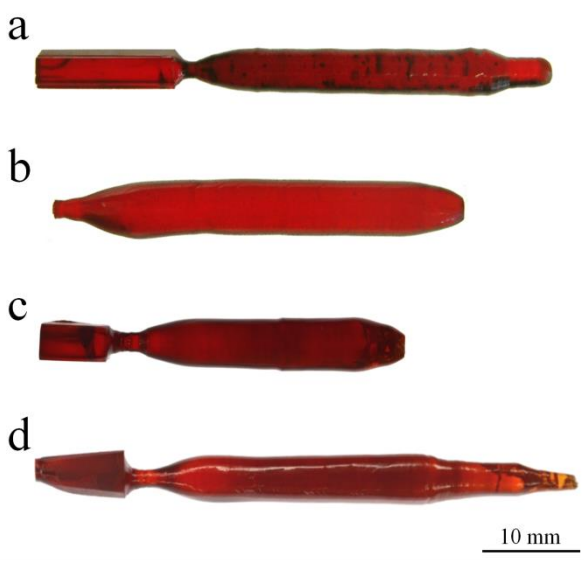

shown in Fig. 2. The growth rate and the rotation rate for every crystal were 2.5 mm/h and 30 rpm, respectively. The as-grown crystals were transparent and deep red in whole. Bubbles of about 1 mm in diameter were observed in the crystals grown in $O_2$ stream as shown in Fig. 2a. The cause of the bubble formation is not yet well known, but pores in the feed rods might be entrained in the molten zone and be trapped at the growth interface. Transparency of the crystal grown in the $N_2$ stream (Fig. 2d) was appreciably lower than those of other crystals grown under different atmospheres. Polarizing microphotographs of the initial portions of the single crystals grown in different atmospheres are shown in Fig. 3. Many voids were found in the central region of every crystal. Much more voids were observed in the crystals grown in the $N_2$ stream and were responsible to the decrease in the transparency of this crystal. The number of voids increased with the progression of crystal growth in every crystal. It was expected that there was some relationship between the oxygen partial pressure and the crystal quality; however, no evident dependence was observed. These results are similar to the previous report by Wang, et al.

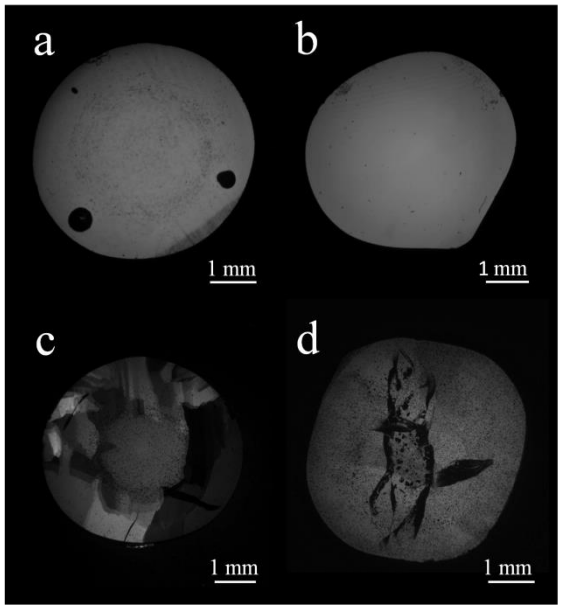

[18]. Although the void formation was not completely suppressed only by controlling the oxygen partial pressure, air was found to be appropriate to grow a better crystal and following results are accordingly obtained by using air as a growth atmosphere.

Fig. 4 shows polarizing microphotographs of the end portions of the crystals grown at different growth rates and rotation rates. Many voids were found in the central regions of the crystal grown at 5 mm/h; however, the number of voids was appreciably reduced in the crystal grown at 2.5 mm/h. Furthermore, increase in the rotation rate from 30 rpm to 60 rpm was also effective to reduce the number of voids.

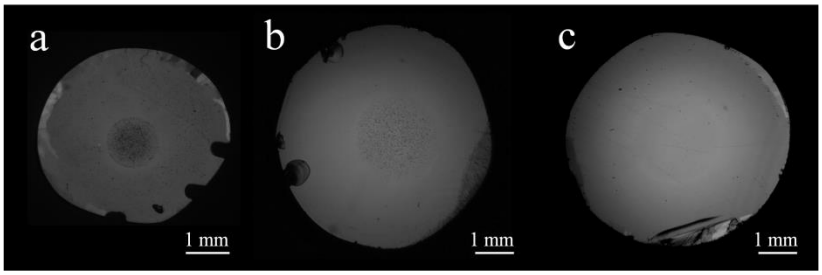


On the basis of above-mentioned results, constitutional super-cooling due to segregation of some chemical species could be responsible to the formation of voids because lower growth rate and higher rotation are effective. In addition this consideration is also supported by the fact that the number of voids increased along the growth direction. In order to identify the chemical species that segregates at the growth interface, lattice parameters of the initial and end portions of the grown crystal (growth rate: 2.5 mm/h, rotation rate: 30 rpm, growth atmosphere: air) were determined from the

X-ray powder diffraction patterns using a least square method. The results are shown in Table 2. The lattice parameters of the end portion are slightly larger than that of the initial portion. Nd or Cr could be the species that segregate since the ionic radii of $Nd^{3+}$ and $Cr^{3+}$ are larger than those of $Y^{3+}$ and $Al^{3+}$, respectively. However, there was no significant difference in the absorption coefficients of the initial and end portions of the crystal and these elements can be excluded. If there is an appreciable difference between the stoichiometric and congruent compositions the elements of the host crystal can be responsible to the segregation.

| | Lattice parameter | |
|---|---|---|
| | a-axis [Å] | c-axis [Å] |
| Initial portion | 3.6455(2) | 11.8750(6) |
| End portion | 3.6471(2) | 11.8813(6) |

As illustrated in Fig. 5, if the congruent composition is shifted from the stoichiometric one towards an end member the ionic radius of which is smaller than that of the counter ion, the increase in the lattice parameter can be explained. On the basis of the ternary phase diagram for the $CaO$-$Y_2O_3$-$Al_2O_3$ system [24], possible

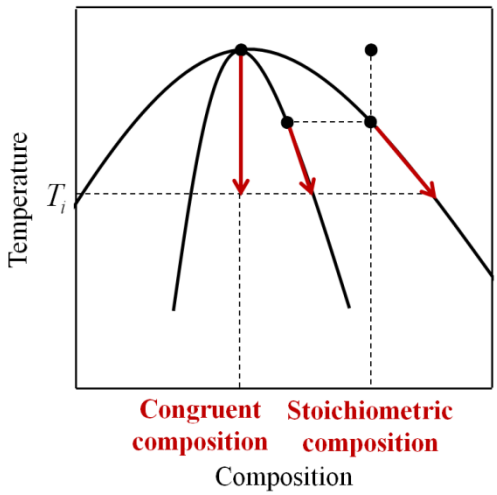

combinations are Al-Y and Y-Ca. The combination of Al-Ca can be excluded since both charges and crystallographic sites are different. Single crystals were accordingly grown using feed rods in which the chemical compositions are Y-rich for Ca (Y/Ca = 1.005/0.9925) and Al-rich for Y (Al/Y = 1.005/0.995). Polarizing microphotographs of the end portions are shown in Fig. 6. While the number of voids in the crystal grown from the feed rod with the Al-rich composition was as many as that in the crystal of the composition, no void was observed in the crystal grown from the Y-rich composition. The quality of the crystal with Y-rich grown at a rotation rate of 30 rpm, was much higher than that of the stoichiometric crystal grown at 60 rpm with the same growth rate of 2.5 mm/h. These results strongly support the anticipation that the void formation is attributable to constitutional super-cooling that is based on segregation between Ca and Y species. Although the true congruent composition of this material is not known, the composition is expected to be around $Ca_{0.9925}(Y,Nd)_{1.005}(Al,Cr)O_4$. If the true congruent composition is determined, higher growth rate than 2.5 mm/h will be possible to obtain high quality Cr,Nd:$CaYAlO_4$ single crystals.

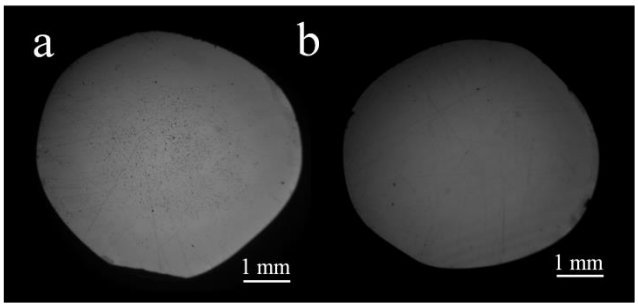

*3.2. Spectroscopic properties*

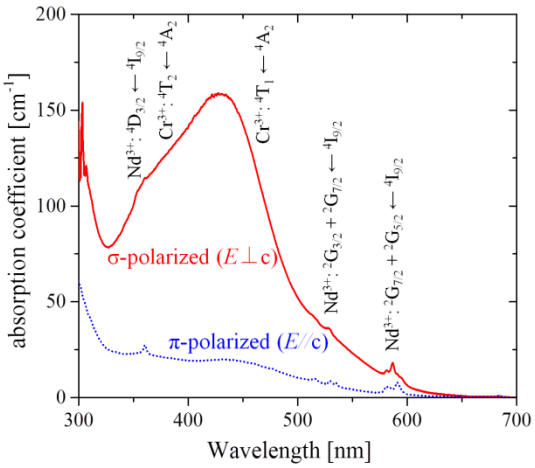


Fig. 7 shows polarized absorption spectra of the Cr,Nd:$CaYAlO_4$ single crystal in the visible region. Strong, broad absorption bands of $Cr^{3+}$ are observed from about 300 nm to 600 nm for the σ-polarization. As expected from the crystal structure in which $AlO_6$ octahedra form layers perpendicular to the c-axis, σ-polarized ($E \perp c$) absorption of $Cr^{3+}$ is larger than the π-polarized ($E//c$) absorption. In contrast, the absorption of $Nd^{3+}$ was independent on the polarization. This is because $Nd^{3+}$ ions substitute the Y-site, in which large anisotropy is not expected as in the Al-site. At 430 nm, which corresponds to the absorption peak of Cr,Nd:YAG, σ-polarized absorption cross-section of Cr,Nd:$CaYAlO_4$ is about 1160 × $10^{-20}$ $cm^2$, which is as 165 times large as that of Cr,Nd:YAG. The absorption peak wavelength of Cr,Nd:$CaYAlO_4$ (428 nm) does not correspond to that of the peak wavelength of the solar radiation (~500 nm); however, the absorption coefficient

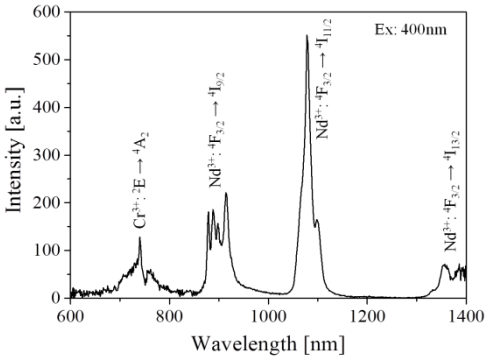

of Cr,Nd:$CaYAlO_4$ at 500 nm is about 50 $cm^{-1}$, which is practically enough for pumping. In addition, appreciable absorption was not observed in the near infrared region, where emission bands of $Nd^{3+}$ exist.

Fig. 8 shows emission spectrum of the Cr,Nd:$CaYAlO_4$ single crystal. Fluorescence bands of $Nd^{3+}$ was observed around 900 nm, 1080 nm and 1400 nm by excitation at 400 nm, where only absorption of $Cr^{3+}$ is present. The fluorescence lifetime which was measured with 370 nm excitation is shown in Fig. 9. Although a little afterglow component was present, the fluorescence lifetime of the Cr,Nd:$CaYAlO_4$ single crystal (growth atmosphere: air, growth rate: 2.5 mm/h, rotation rate: 30 rpm) is 132 μs. The fluorescence spectrum and lifetime are similar to the previous studies [15, 17].These results indicate that energy transfer from $Cr^{3+}$ to $Nd^{3+}$ occurs in the Cr,Nd:$CaYAlO_4$ single crystal.

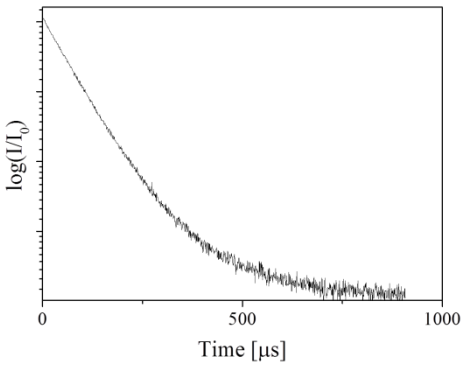


## 4. Conclusion

In this study, we focused on Cr,Nd:$CaYAlO_4$ as a candidate of gain media for solar-pumped laser, and grew Cr,Nd:$CaYAlO_4$ single crystals by the floating zone

method. In order to obtain a high-quality crystal following growth conditions were examined: growth atmosphere, growth rate, rotation rate, and compositions of the feed rod. Lower growth rate, higher rotation rate and air atmosphere were effective to improvement the crystal quality, and a void free Cr,Nd:$CaYAlO_4$ single crystal was obtained by using a feed rod with the Y-rich composition (Ca/Y = 0.9925/1.005). Void formation is attributable to constitutional super-cooling based on the segregation between Ca and Y species. From the polarized absorption spectra of the Cr,Nd:$CaYAlO_4$, the σ-polarized absorption cross-section of Cr,Nd:$CaYAlO_4$ is $1160 \times 10^{-20}$ $cm^2$, which is as 165 times large as that of Cr,Nd:YAG at 430 nm. Emission bands of $Nd^{3+}$ were observed around 900 nm, 1080 nm and 1400 nm with the excitation at 400 nm indicating energy transfer from $Cr^{3+}$ to $Nd^{3+}$ in the Cr,Nd:$CaYAlO_4$ single crystal. The fluorescence lifetime was 132 μs. For all of these reasons, Cr,Nd:$CaYAlO_4$ single crystals are a promising material as a gain medium for solar-pumped laser systems.

**References**


[1] T. Yabe, S. Uchida, K. Ikuta, K. Yoshida, C. Baasandash, M.S. Mohamed, Y. Sakurai, Y. Ogata, M. Tuji, Y. Mori, Y. Satoh, T. Ohkubo, M. Murahara, A. Ikesue, M. Nakatsuka, T. Saiki, S. Motokoshi, C. Yamanaka, J. Appl. Phys., 89 (2006) 261107, doi: 10.1063/1.2423320

[2] T. Yabe, B. Bagheri, T. Ohkubo, S. Uchida, K. Yoshida, T. Funatsu, T. Oishi, K. Daito, M. Ishioka, N. Yasunaga, Y. Sato, C. Baasandash, Y. Okamoto, K. Yanagitani, J. Appl. Phys., 104 (2008) 083104, doi: 10.1063/1.2998981

[3] T. Okada, T. Saiki, S. Taniguchi, T. Ueda, K. Nakamura, Y. Nichikawa, Y. Iida, ISRN Renewable Energy, vol. 2013 (2013) 827681

[4] F. Zhang, A. Yamakata, K. Maeda, Y. Moriya, T. Takata, J. Kubota, K. Teshima, S. Oishi, K. Domen, J. Am. Chem. Soc., 134 (2012) 8348

[5] M. Mori, H. Kagawa, Y. Saito, Acta Astronautica, 59 (2006) 132

[6] T. Suzuki, H. Nasu, M. Hughes, S. Mizuno, K. Hasegawa, H. Ito, Y. Ohishi, J. Non-Cryst. Solids, 356 (2010) 2344

[7] T. Suzuki, H. Kawai, H. Nasu, M. Hughes, Y. Ohishi, S. Mizuno, H. Ito, K. Hasegawa, Opt. Mater., 33 (2011) 1952

[8] C.G. Young, Appl. Opt., 5 (1966) 993

[9] M. Weksler, J. Shwartz, J. Quant. elect., 24 (1988) 1222

[10] H. Arashi, Y. Oka, N. Sasahara, A. Kanai, M. Ishigame, Jap. J. Appl. Phys., 23 (1984) 1051

[11] T. Yabe, T. Ohkubo, S. Uchida, K. Yoshida, M. Nakatsuka, T. Funatsu, A. Mabuti, A. Oyama, K. Nakagawa, T. Oishi, K. Daito, B. Behgol, Y. Nakayama, M. Yoshida, S. Motokoshi, Y. Sato, C. Baasandash, Appl. Phys. lett., 90 (2007) 261120, doi: 10.1063/1.2753119

[12] T. Saiki, M. Nakatsuka, K. Imasaki, Jap. J. Appl. Phys., 49 (2010) 082702

[13] S.Q. Li, S.H. Zhou, P. Wang, Y.C. Chen, K.K. Lee, Opt. Lett., Vol. 18, No. 3 (1993) 203

[14] J.P. Oudalov, A. Daoudi, JC. Joubert, G.L. Flem, P. Hagenmuller, Bull. Soc. Chim. Fr., 10 (1970) 3408

[15] H.R. Verdun, L.M. Thomas, Appl. Phys. Lett., 56 (1990) 608

[16] D.H. Cong, D.Y. Tang, W.D. Tan, J. Zhang, D.W. Luo, C.W. Xu, X.D. Xu, D.Z. Li, J. Xu, X.Y. Zhang, Q.P. Wang, Opt. Comm., 286 (2011) 1967

[17] D.Z. Li, X.D. Xu, J. Meng, D.H. Zhou, C. Xia, F. Wu, J. Xu, Optics Express, 18 (2010) 18649

[18] W.Y. Wang, X.L. Yan, X. Wu, Z.G. Zhang, B.Q. Hu, J.F. Zhou, J. Cryst. Growth,

219 (2000) 56

[19] J.Q. Di, X.D. Xu, C.T. Xia, D.Z. Li, D.H. Zhou, Q.L. Sai, L. Wang, J. Xu, Physica B: Condens. Matter, 408 (2013) 1

[20] S.Z. Lv, Z.J. Zhu, Y. Wang, Z.Y. You, J.F. Li, C.Y. Tu, J. Lumin., 144 (2013) 117

[21] J.A. Hutchnson, H.R. Verdun, B.H.T. Chai, B. Zandi, L.D. Merkle, Opt. Mater., 3 (1994) 287

[22] M. Yamaga, P.I. Macfarlane, K. Holliday, B. Henderson, N. Kodama, Y. Inoue, J. Phys.: Condens. Matter, 8 (1996) 3487

[23] T. Stoyanova Lyubenova, J.B. Carda, M. Ocana, J. Eur. Ceram. Soc., 29 (2009) 2193

[24] Yu.P. Udalov, Z. S. Appen, V.V. Parshina, Zh. Neorg. Khim., 24 (1979) 2786; Russ. J. Inorg. Chem. (Engl. Transl.), 24 (1979) 1549.

Table 1

Compositions of feed rods used for growth experiments.

| Sample | Composition |
|---|---|
| Stoichiometry | $Ca(Y_{0.99}Nd_{0.01})(Al_{0.999}Cr_{0.001})O_4$ |
| Y-rich 0.5 mol% vs. Ca | $Ca_{0.9925}(Y_{0.99}Nd_{0.01})_{1.005}(Al_{0.999}Cr_{0.001})O_4$ |
| Al-rich 0.5 mol% vs. Y | $Ca(Y_{0.99}Nd_{0.01})_{0.995}(Al_{0.999}Cr_{0.001})_{1.005}O_4$ |

Table 2

Lattice parameters of the initial and end portions of the grown crystal.

| | Lattice parameter | |
|---|---|---|
| | a-axis [Å] | c-axis [Å] |
| Initial portion | 3.6455(2) | 11.8750(6) |
| End portion | 3.6471(2) | 11.8813(6) |

**Figure captions**

Fig. 1 Crystal structure of $CaYAlO_4$.

Fig. 2 Cr,Nd:$CaYAlO_4$ crystals grown under different atmospheres; a: $O_2$; b: air; c: mixed gas ($N_2$/air = 9/1); d: $N_2$. All crystals were grown at 2.5 mm/h and 30 rpm.

Fig. 3 Polarizing microphotographs of the of the initial portions of the Cr,Nd:$CaYAlO_4$ crystals grown under different atmospheres. a: $O_2$; b: air; c: mixed gas ($N_2$/air = 9/1); d: $N_2$. All crystals were grown at 2.5 mm/h and 30 rpm.

Fig. 4 Polarizing microphotographs of the end portions of the Cr,Nd:$CaYAlO_4$ crystals grown at different growth rates and rotation rates. a: 5 mm/h, 30 rpm; b: 2.5 mm/h, 30 rpm; c: 2.5 mm/h, 60 rpm. All crystals were grown in air.

Fig. 5 Schematic phase diagram in which the stoichimetric composition and the congruent one are different If the congruent composition is shifted from the stoichimetric one towards an end member, the ionic radius of which is smaller than that of the counter ion, the lattice parameter will increase.

Fig. 6 Polarizing microphotographs of the end portions of the Cr,Nd:$CaYAlO_4$ crystals grown from feed rods with different compositions. a: Al-rich

composition (Y/Al = 0.995/1.005); b: Y-rich composition (Ca/Y = 0.9925/1.005). Compare the qualities with that of the stoichiometric one shown in Fig. 4b. Every crystal was grown at 2.5 mm/h and 30 rpm in air.

Fig. 7 Polarized absorption spectra of the Cr,Nd:$CaYAlO_4$ single crystal.

Fig. 8 Emission spectrum of the Cr,Nd:$CaYAlO_4$ single crystal with the excitation at 400 nm.

Fig. 9 Fluorescence decay curve of 1078 nm emission of Cr,Nd:$CaYAlO_4$ at room temperature. Excited wavelength was 370 nm, where only absorption fo $Cr^{3+}$ is present.